Performance of Non-Coherent FSK Virtual MISO Systems in Correlated Rayleigh Fading

Muddassar Hussain and Syed Ali Hassan

School of Electrical Engineering & Computer Science (SEECS)
National University of Sciences & Technology (NUST), 44000, Islamabad, Pakistan

***Abstract*— In this paper, a virtual multiple-input single-output (VMISO) network employing non-coherent frequency shift keying (FSK) is considered. In the VMISO network, spatially separated single-antenna nodes transmit the same information cooperatively to a single receiver where the transmitted signals propagate via correlated Rayleigh fading channel. The effects of the channel correlation on the performance of the system are analyzed. Specifically, we determine the statistics of the decision variables of FSK receiver and derive the closed-form expression for the probability of symbol error. The results indicate a degradation in performance due to channel correlation. Therefore, an extra SNR margin or higher array gain is required to compensate the performance degradation because the channel correlations.**

***Index Terms*— Non-coherent frequency shift keying (FSK), wireless sensor networks (WSNs), correlated fading, equal gain combining (EGC).**

I. Introduction

Cooperative transmission (CT) is an emerging paradigm in wireless communication, which combats the effects of multipath fading by employing spatial diversity. CT has become a promising candidate for wireless sensor networks (WSNs) because of its inherent advantages such as energy-efficiency and range extension [1–3]. Since the transceivers for WSNs should be cost-effective and energy-efficient, a low-complexity modulation scheme is desirable [4]. One such scheme is non-coherent frequency shift keying (FSK), with many advantages such as constant signal envelope, efficient amplification at the transmitter, and a simple receiver design employing energy detection. Because radios in WSNs are low-powered, non-coherent FSK scheme is used along with non-coherent combining techniques such as equal gain combining (EGC) to provide array gain and range extension [5].

The effects channel correlation on the performance of FSK systems are previously studied in [6] and [7]. In [6], the performance of non-coherent FSK system employing the post-detection selection diversity is analyzed. The results are provided for both Rayleigh and Rice fading with arbitrary correlation. In [7], a non-coherent FSK system operating in correlated Nakagami fading environment is considered, which uses post-detection EGC. The authors have derived the expression for probability of symbol error. The results depict a performance degradation due to channel correlation.

In this paper, we consider a non-coherent FSK virtual multiple-input single-output (VMISO) system employing pre-detection non-coherent EGC. The transmitting nodes send the same message to the receiver node via flat and slow Rayleigh fading channel where channel is coefficients are correlated. We aim to quantify the effects of channel correlation on the probability of symbol error, which in turns can be used as pre-condition for forwarding the data to the next hop in a multi-hop CT network. Since the decoding in each node is independent of one-another, we focus on finding error probability at a single receiver; which would be identical in each receiving node of the cooperative multi-hop network.

II. System Model

Consider a VMISO communication system with K transmitting nodes employing orthogonal M-ary frequency shift keying (M-FSK) modulation with non-coherent detection. The signal transmitted by each transmitting node is given as

$$s_m(t) = \sqrt{\frac{E_s}{T}} \exp(j2\pi(f_c + f_m)t), \quad 0 \le t \le T, \quad m \in \{1, 2, \ldots, M\}, \quad M = 2^N, N \in \mathbb{Z}^+ \tag{1}$$

where E_s is the signal energy, T is symbol period, f_c is the carrier frequency and f_m is the M-FSK frequency corresponding to the m^{th} transmitted symbol. All K nodes relay the same message signal to a single receiver through correlated fading channels and the received signal after non-coherent EGC is given as

$$r(t) = \sqrt{\frac{E_s}{T}} \sum_{k=1}^{K} h_k \exp(j2\pi(f_c + f_m)t) + n(t), \tag{2}$$

where $n(t)$ denotes the additive white Gaussian noise (AWGN) having single-sided power spectral density N_o W/Hz. The h_k denotes the channel coefficient between the k^{th} transmitter and the receiver, corresponding to flat Rayleigh channel, which is assumed to follow a complex normal distribution with zero mean and unit variance, i.e., $\mathbb{E}[|h_k|^2] = 1$, $\forall k$. The channel coefficients exhibit correlation, which follows the model given in [8]. In the

This work was supported by the National ICT R&D Fund, Pakistan.

subsequent section, the expression of probability of symbol error is derived.

III. Average Probability of Symbol Error

Upon reception, the signal is passed through a correlator receiver and the correlator output is given as

$$x_m = \int_0^T r(t)\sqrt{\frac{E_s}{T}}\exp(j2\pi(f_c+f_m)t)dt, \tag{3}$$

where the subscript m denotes the m^{th} branch of the receiver. Without the loss of generality, we assume that s_1 is the transmitted symbol. Therefore, the first branch of the receiver contains data and other branches contain noise only. The signal in the first branch before envelope detection is given as

$$x_1 = E_s\sum_{k=1}^{K} h_k + n_1, \tag{4}$$

whereas the signal in the rest of branches is simply $x_i = n_i,\ i = \{2,3,\ldots,M\}$. The noise terms $n_m,\ \forall m$ are complex Gaussian with zero mean and E_sN_o variance. After passing through correlator, the signals are applied to the square law detectors whose outputs are given as

$$y_1 = \left|E_s\sum_{k=1}^{K} h_k + n_1\right|^2, \quad y_i = |n_i|^2, i = \{2,3,\ldots,M\}. \tag{5}$$

Because $x_m,\ \forall m$ are independent complex Gaussain RVs, therefore, $y_m,\ \forall m$ become independent exponential RVs. The receiver's decision is based on selecting the maximum of the $y_m,\ \forall m$. Assuming that s_1 is transmitted, the probability of symbol error of the system is given as

$$P_e = 1 - \Pr(y_2 < y_1, y_3 < y_1, \ldots, y_M < y_1). \tag{6}$$

To get the expression of probability of symbol error, the statistics of $y_m,\ \forall m$ are required. For that purpose, we denote the correlation coefficient matrix between the channel coefficients $h_k\ \forall k$ by $\mathbf{R}$, $\mathbf{R}_{ij} = \rho_{i,j},\ i,j = \{1,2,\ldots,K\}$, where

$$\rho_{i,j} = \frac{\mathbb{E}\left[h_i h_j^*\right]}{\sqrt{\mathbb{E}\left[|h_i|^2\right]\mathbb{E}\left[|h_j|^2\right]}} = \mathbb{E}\left[h_i h_j^*\right]. \tag{7}$$

The first moment of y_1 is given as

$$\lambda_1 = \mathbb{E}[y_1] = E_s^2\mathbb{E}\left[\left|\sum_{k=1}^{K} h_k\right|^2\right] + \mathbb{E}[|n_1|^2] + E_s\mathbb{E}\left[n_1^*\sum_{k=1}^{K} h_k\right] + E_s\mathbb{E}\left[n_1\sum_{k=1}^{K} h_k^*\right]. \tag{8}$$

The third and fourth terms in (8) contain expected value of noise, which is zero. Therefore, (8) can be written as

$$\lambda_1 = E_s^2\mathbb{E}\left[\left|\sum_{k=1}^{K} h_k\right|^2\right] + E_sN_o. \tag{9}$$

After expanding the first term in (9), we get

$$\lambda_1 = E_s^2\mathbb{E}\left[\sum_{k=1}^{K}|h_k|^2\right] + E_s^2\mathbb{E}\left[\sum_{i=1}^{K}\sum_{\substack{j=1\\ i\neq j}}^{K} h_i hj^*\right] + E_sN_o. \tag{10}$$

After applying the expected value, the final expression of λ_1 is found, which is given as

$$\lambda_1 = KE_s^2 + E_s^2\sum_{i=1}^{K}\sum_{\substack{j=1\\ i\neq j}}^{K}\rho_{i,j} + E_sN_o. \tag{11}$$

The first moment of $y_i,\ i = \{2,3,\ldots,M\}$ is simply given by

$$\lambda = \mathbb{E}[y_i] = E_sN_o, \qquad i = \{2,3,\ldots,M\}. \tag{12}$$

Now consider the following theorem.

Theorem 1. *For a K node VMISO system employing non-coherent orthogonal M-FSK with EGC, the probability of symbol error in correlated Rayleigh fading environment is given as*

$$P_e = 1 - \frac{\zeta\Gamma(M)\Gamma(\zeta)}{\Gamma(\zeta+M)}, \tag{13}$$

where

$$\zeta = \frac{1}{K\gamma + \gamma\sum_{i=1}^{K}\sum_{\substack{j=1\\ i\neq j}}^{K}\rho_{i,j} + 1}, \quad \gamma = \frac{E_s}{N_o}. \tag{14}$$

and $\Gamma(.)$ is Euler Gamma function.

Proof: From (6), the probability of symbol error is given as

$$\begin{aligned} P_e &= 1 - \Pr(y_2 < y_1, y_3 < y_1, \ldots, y_M < y_1) \\ &= 1 - \int_0^\infty \Pr(y_2 < y, y_3 < y, \ldots, y_M < y) f_{y_1}(y)dy \\ &= 1 - \int_0^\infty F_{y_2,y_3,\cdots,y_M}(y) f_{y_1}(y)dy, \end{aligned} \tag{15}$$

where $F_{y_2,y_3,\cdots,y_M}(y)$ is the joint cumulative density function (CDF) of i.i.d exponential RVs $y_2, y_3, \ldots, y_M$, which is given as

$$F_{y_2,y_3,\cdots,y_M}(y) = \prod_{m=2}^{M} F_{y_m}(y) = \left(1-\exp\left(-\frac{y}{\lambda}\right)\right)^{M-1}. \tag{16}$$

In (15), $f_{y_1}(y)$ is the probability density function (PDF) of y_1, which is given as

$$f_{y_1}(y) = \frac{1}{\lambda_1}\exp\left(-\frac{y}{\lambda_1}\right). \tag{17}$$

Substituting from (16) and (17) into (15), gives

$$\begin{aligned} P_e &\overset{(a)}{=} 1 - \int_0^\infty \frac{1}{\lambda_1}\left(1-\exp\left(-\frac{y}{\lambda}\right)\right)^{M-1}\exp\left(-\frac{y}{\lambda_1}\right)dy \\ &\overset{(b)}{=} 1 - \int_0^1 \frac{\lambda}{\lambda_1} z^{M-1}(1-z)^{\frac{\lambda}{\lambda_1}-1}dz \\ &\overset{(c)}{=} 1 - \frac{\lambda\Gamma\left(\frac{\lambda}{\lambda_1}\right)\Gamma(M)}{\lambda_1\Gamma\left(\frac{\lambda}{\lambda_1}+M\right)}, \end{aligned} \tag{18}$$

where (b) is obtained after applying variable transformation, $y = -\lambda\ln(1-z)$ in (a), and (c) is found after solving integration in (b). After substituting the values λ_1 and λ from (11) and (12) into (18), the expression for probability of symbol error is found, which is given in (13). ■

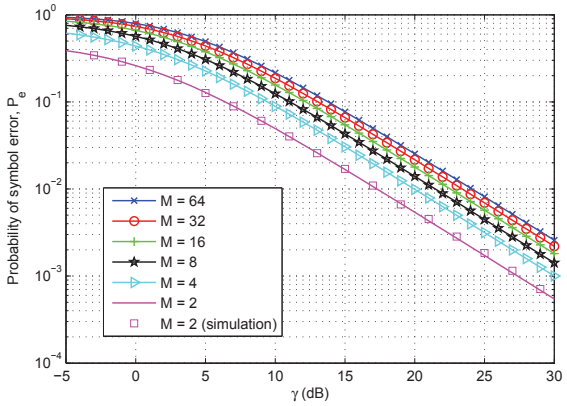

Fig. 1. The probability of symbol error against SNR for different orders of FSK, M; $K = 3$.

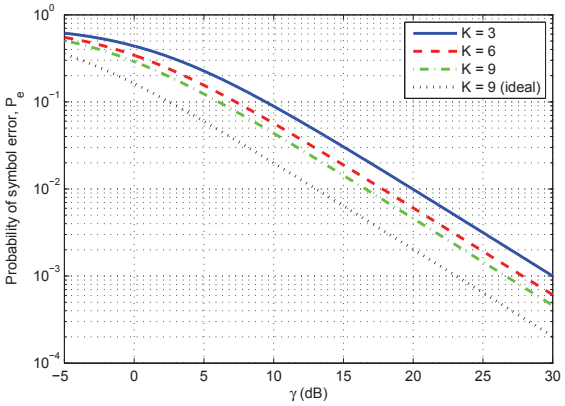

Fig. 2. The probability of symbol error against different number of transmitting nodes, K; $M = 4$.

IV. Results and System Performance

In this section, the simulation and analytical results for the VMISO FSK system are provided. The simulation results are obtained using Monte-Carlo with 10^5 iterations for each simulation point. We use the Cholesky decomposition of matrix $\mathbf{R}$ to get a upper triangular matrix $\mathbf{C}$, such that $\mathbf{C}^T\mathbf{C} = \mathbf{R}$. This matrix is used to generate the correlated complex Gaussian RVs h_k $\forall k$ using $\mathbf{h} = \tilde{\mathbf{h}}\mathbf{C}$, where $\tilde{\mathbf{h}}$ is vector of uncorrelated channel coefficients and $\mathbf{h} = [h_1\ h_2 \cdots h_K]$. The transmitting nodes are assumed to be deployed in a line with equal spacing between consecutive nodes. The correlation coefficients are obtained using the correlation model given in [8, Eq.(2.2.6)].

In Fig. 1, a plot of probability of symbol error, P_e versus the SNR and for different orders of FSK, M, is shown. It can be noticed that the probability of symbol error decreases in monotonic fashion as SNR is increased. A simulation curve is also shown in the figure for $M = 2$, which matches with the corresponding analytical curve. A saturation trend can observed for the probability of symbol error as M is increased, i.e., the increase in P_e is maximum from $M = 2$ to $M = 4$ and is minimum for $M = 32$ to $M = 64$. A tradeoff can be observed between the SNR margin and using higher order FSK. For instance, to increase data rate by 4 times, an extra SNR margin of 5dB has to be provided for $M = 16$ as compared to $M = 2$ to maintain the same probability of symbol error.

Fig. 2 shows the probability of symbol error versus SNR for different number of transmitting nodes, K and $M = 4$. As previously, a monotonic trend is followed by the probability of symbol error. Comparing the curves for different values of K, it can be seen that the probability of symbol error decreases as K is increased. This is because of the enhanced array gain for higher K. We have shown an ideal case for $K = 9$, in which channel correlation is taken to be zero. Comparing this ideal case with the corresponding correlated case, we can see a deterioration in performance as large as 4 dB due to channel correlation. This result is useful in the decode-and-forward sense where the receiver forwards the message only if the P_e remains less than a specified threshold. For instance, if $P_e \leq 10^{-2}$ is required to successfully decode and forward the information to next hop, then 20dB of SNR is required to obtain this performance for $K = 3$. Another choice will be to use $K = 9$, however, the SNR requirement goes down to 16dB.

V. Conclusion

In this paper, we have considered a virtual MISO system employing non-coherent FSK with pre-detection EGC. We have analyzed the effects of channel correlation on the performance of the system. Specifically, we have derived the closed-form expression of the probability of symbol error. A degradation in performance has been observed due to channel correlation and an extra SNR margin required to compensate the performance degradation is quantified.

References

[1] A. Afzal and S. A. Hassan, "Stochastic modeling of cooperative multi-hop strip networks with fixed hop boundaries," *IEEE Trans. Wireless Commun.*, vol. 13, no. 8, pp. 4146–4155, Aug. 2014.

[2] M. Hussain and S. A. Hassan, "Analysis of bit error probability for imperfect timing synchronization in virtual MISO networks," in *Proc. IFIP Wireless Days (WD)*, Nov. 2014.

[3] M. Hussain and S. A. Hassan, "Imperfect timing synchronization in multi-hop cooperative networks: statistical modeling and performance analysis," in *Proc. IFIP Wireless Days (WD)*, Nov. 2014.

[4] J. Abouei, K. N. Plataniotis, and S. Pasupathy, "Green modulations in energy-constrained wireless sensor networks," *IET Commun.*, vol. 5, no. 2, pp. 240–251, 2011.

[5] G. Farhadi and N.C. Beaulieu, "A low complexity receiver for non-coherent amplify-and-forward cooperative systems," *IEEE Trans. Commun.*, vol. 58, pp. 2499–2504, Sept. 2010.

[6] S. Haghani and N.C. Beaulieu, "Performance of S+N selection diversity receivers in correlated Rician and Rayleigh fading," *IEEE Trans. Wireless Commun.*, vol. 7, no. 1, pp. 146–154, Jan. 2008.

[7] M.Z. Win and R.K. Mallik, "Error analysis of noncoherent M-ary FSK with postdetection EGC over correlated Nakagami and Rician channels," *IEEE Trans. Commun.*, vol. 50, no. 3, pp. 378–383, Mar. 2002.

[8] G. L. Stuber, "Principles of Mobile Communication," 3rd Ed. in *Springer*, Sept. 2011.